JOURNAL OF CATALYSIS 101, 342–351 (1986)

Platinum-Catalyzed Hydrogenation of Graphite: Mechanism Studied by the Rates of Monolayer Channeling

PETER J. GOETHEL AND RALPH T. YANG

Department of Chemical Engineering, State University of New York, Buffalo, New York 14260

Received February 27, 1986; revised May 8, 1986

Monolayer channeling on the basal plane of graphite was studied for the Pt-catalyzed C–H_2 reaction using gold decoration transmission electron microscopy, at temperatures below 1050°C, H_2 pressures below 1 atm, and Pt particle sizes below 5000 Å. The particle movement is driven by the adhesion forces between Pt and the $\{10\bar{1}1\}$ zigzag edge plane of graphite. Larger particles channel faster but the gasification rate per Pt surface area is the same for all sizes. The rate is independent of H_2 partial pressure. The kinetic data suggest that the rate-limiting step is the reaction on the Pt surface between surface carbon and chemisorbed hydrogen at their equilibrium amounts. A comparison of the monolayer channeling data and those on multilayer channeling and bulk measurement indicates that there exists a similarity between the mechanisms. A further comparison of the kinetic data for the catalyzed C–H_2 reaction and for the methanation reaction (from CO + H_2) suggests the likelihood of a common rate-limiting step.

INTRODUCTION

The active carbon atoms in the uncatalyzed graphite gasification reactions are the atoms on the crystal steps, edges, and imperfections on the surface, having an unpaired sp^2 electron. It has become clear in the last decade that the same active atoms are also responsible for the solid-catalyzed carbon gasification reactions. The situation here is much more complex due to the existence of a second solid (catalyst) which usually exists in the form of fine particles that are in contact with the carbon.

It has been established, primarily by Baker and co-workers using controlled-atmosphere electron microscopy (e.g., Ref. (*1*)), that the catalyst acts mainly by carving channels in graphite and coating edges at the graphite layers to promote edge recession. All channels initiate at the steps and edges. The dominant mode of catalyst action depends on the wetting condition, which in turn depends on the gas environment and temperature. The catalytic actions are propagated by adhesion forces; the catalyst is active when it wets the graphite surface, vis-a-vis

$$\gamma_{\text{catalyst/graphite}} < \gamma_{\text{gas/graphite}}$$

where γ is the interfacial tension.

The predominant product for the carbon–hydrogen reaction is methane at temperatures below about 1800 K (*2*). Studies of the carbon–hydrogen reaction catalyzed by Group VIII metals (*3, 4*), and in particular by nickel (*5–8*), have been reported. Using a gravimetric technique Rewick *et al.* (*9*) studied the platinum-catalyzed hydrogenation reaction and suggested a hydrogen spillover mechanism. It was later shown by Holstein and Boudart (*2*) that the true reaction order with respect to hydrogen was zero for the platinum-catalyzed reaction, using a fixed-bed differential reactor. They suggested that the rate-limiting step is the carbon–carbon bond breakage at the metal–carbon interface. The reaction was studied in the temperature range of 560–800°C at hydrogen partial pressures below 1 atm. The same reaction was studied using the controlled atmosphere TEM technique by Baker *et al.* (*10*) at 845–1230°C and 1 Torr hydrogen for the channeling action of platinum. The conclusion drawn from this study, as well as from the studies on the

0021-9517/86 $3.00

nickel-catalyzed reaction (*5, 6*), was that the rates were proportional to the surface area of the metal as larger particles channeled at higher speeds, indicating a surface reaction limited rate process.

The channels visualized in the controlled atmosphere TEM studies are many layers deep and are thus visible due to thickness contrast. These channel depths cannot be accurately determined. However, with monolayer (3.35 Å deep) etch pits and channels, which can be visualized only with the aid of gold decoration, the depth is exactly known thus resulting in accurate calculation of rates. The gold decoration TEM technique, originally invented by Hennig (*11*), has helped significantly in our understanding of the uncatalyzed gas–carbon reactions (see reviews in (*11–13*)). The gold decoration technique was used in this investigation to study the mechanism of the platinum-catalyzed monolayer channeling in the graphite–hydrogen reaction. Although monolayer channeling does not significantly contribute to the total gasification rates, its mechanism is the same as that for deep-layer channeling, as will become apparent below.

EXPERIMENTAL

The carbon used in this study was a natural single crystal graphite from Ticonderoga, New York. This graphite was employed due to its well-defined crystalline structure and ability to be cleaved into specimens thin enough for transmission electron microscope (TEM) observation while maintaining a large single crystal basal plane area. The techniques used to prepare the samples for TEM observation have been explained in full by Wong (*14*).

The technique of gold decoration was used to make visible the single-layer (3.35 Å depth) steps on the basal plane of graphite. Thus the kinetics of the monolayer channeling could be followed. The details of this technique were explained elsewhere (*14*).

The platinum catalyst was deposited on the sample by means of vacuum evaporation. The samples were placed on a glass slide, and slotted electron microscope grids were placed over the samples which provided bare areas on the basal plane for reaction. The platinum source was 99.99% pure wire from Ladd Industries. A triple woven tungsten V-filament was used as the evaporation source. A platinum thickness of 400 Å was deposited, assuming spherical evaporation. Upon heating in hydrogen the Pt islands rapidly dispersed into small particles at temperatures higher than ca. 700°C.

The catalyzed carbon–hydrogen reaction was carried out in a quartz tube which was heated by a split tube furnace. The partial pressure of hydrogen was regulated by controlling the flow rates of the hydrogen and helium carrier streams. The temperature was controlled by an Omega controller with a thermocouple probe inserted inside the quartz tube and located in close proximity to the sample. The samples were placed on a saphire plate and then in a glazed porcelain combustion boat before being placed inside the reactor. The gas purification and reaction preflush heatup were found to be crucial factors in these monolayer channeling experiments.

In a separate study conducted in our laboratory it was found that the ultrahigh purity hydrogen (99.999% minimum) and the ultrahigh purity helium (99.999% minimum) contained levels of O_2, H_2O, and CO_2 high enough to cause uncatalyzed reactions, thus producing etch pits at temperatures as low as 850°C (*16*). A high residence time liquid-N_2 trap was designed which employed three separate beds of activated carbon, 13X zeolite and 5A zeolite. This purifier eliminated etch pits with any traces of impurity up to temperatures of 1100°C.

It was important to pretreat the sample with hydrogen. Without the hydrogen pretreatment, the surface oxide on platinum was found to destroy the integrity of the basal plane by creating etch pits surrounding the Pt. This can be seen in TEM pictures (*16*), where an oxidation reaction has

removed many basal planes of graphite directly beneath the platinum. The destruction of the basal plane left the sample unsuitable for studying the propagation of monolayer channels. This oxide reaction was removed by slowly heating up the sample in a hydrogen atmosphere, thus reducing the platinum surface and removing the oxygen, before a temperature necessary for the carbon–oxygen reaction to occur was reached. This removal of oxide reaction is evident in TEM pictures where the gold nucleated on the edge of the platinum showed no oxide reaction eminating from the platinum (*16*).

Following the hydrogen reduction pretreatment, the samples were then heated in 100% He to the desired reaction temperature. The hydrogen and helium flows were then adjusted to obtain the desired partial pressure of hydrogen. The gas flow was switched back to pure helium after completing the reaction and the reactor was turned off. The split tube furnace was opened, allowing the samples to cool from the reaction temperature to less than 200°C in under 5 min.

The samples were next decorated with gold and placed in a JEOL-100U TEM for observation. The TEM micrographs were used to measure the length and width of the monolayer channels. Only those channels originating at lattice vacancies could be considered monolayer channels with confidence. The diameter of the particles were also measured from the micrographs. The orientations of the decorated edges and steps were determined by selected-area electron diffraction (*14*). The experimental variables were reaction temperature and hydrogen partial pressure. Control experiments were performed to show that there were no gas impurity effects as well as to prove that gasification rate was not a function of reaction time.

RESULTS AND DISCUSSION

The basal plane of the graphite sample contains vacancies at densities of 1–20 μm^{-2} (*15*). When exposed to reactive gases such as O_2, CO_2, and H_2O the vacancies are expanded into monolayer etch pits which can be visualized in TEM with gold decoration (*11–15*). Exposure of the basal plane, without deposited catalyst, to 1 atm H_2 (rigorously purified for 10 h) at temperatures up to 1050°C produced no etch pits (*16*). (Etch pits were produced, however, with "Ultrahigh Purity" hydrogen that was used as received.)

The question of whether the hydrogen spillover mechanism was operative on the platinum deposited basal plane of graphite was then studied. In the $Pt/C/H_2$ system spillover would be the dissociative adsorption of hydrogen on platinum followed by migration of hydrogen atoms across the platinum–carbon interface to the basal plane of carbon. The diffusion of hydrogen atoms across the basal plane to reactive sites such as lattice vacancies and dislocations then follows. Experiments were conducted at temperatures ranging from 400 to 1050°C to search the basal plane for etch pits. No pits were found. Atomic hydrogen is highly reactive to edge carbon sites creating etch pits with a turnover frequency of 32.6 s^{-1} at 717°C (*17*). Thus it is concluded that hydrogen spillover is not operative on the graphite basal plane.

Monolayer Channeling: Origins

The viewing of Pt-deposited samples reacted with H_2 at temperatures of 850°C and higher revealed the formation of shallow channels on the basal plane. Such channels are not detectable without gold decoration. Deep channels at various depths were also seen but will not be discussed in this work.

Two types of shallow channels are created on the basal plane by platinum particles, as illustrated in Fig. 1. One type is originated at the single vacancies in the basal plane while the other is originated at the step of the ledge. The monolayer etch pits originating from single vacancies have been extensively studied (*11–15*). That the vacancy-originated etch pits are indeed mono-

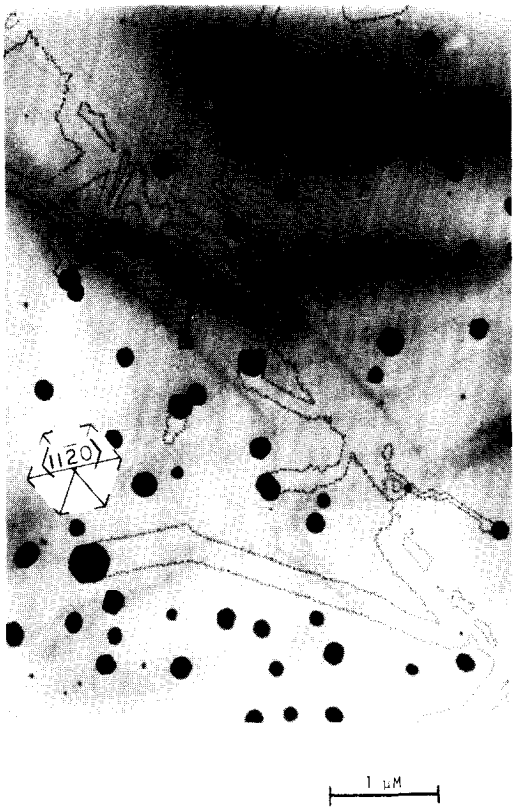

FIG. 1. Platinum particles channeling at 850°C in 1.0 atm hydrogen for 45.0 min. This shows a step in the basal plane to be a reactive site which initiates channels.

layer in depth has been elaborately shown by Hennig (*18*). As illustrated in Fig. 1, the shallow channels do not change depth during channeling by the Pt particle. Figures 2 and 3 show, respectively, vacancy-originated channels before and after crossing paths. The merging pattern provides further evidence that the vacancy-originated channels are monolayer in depth. It has been found in the uncatalyzed graphite–oxygen reaction studies that a substantial amount of monolayer ledges remain on the basal after sample cleavage (*19*). The channels originated at the ledge shown in Fig. 1 are also monolayer in depth. It is apparent that the ledge is also monolayer in depth.

Orientations for Channel Propagation

The orientations of monolayer channeling is essentially the same as those for deep layer channeling (*3, 5–7, 10*). The platinum particle can channel in either the ⟨11$\bar{2}$0⟩ (parallel to the zigzag face) or ⟨10$\bar{1}$0⟩ (parallel to the armchair face) directions, as shown in Fig. 4. It is important to note, however, that the faceted orientation of the leading front of the channel remained the same in both channeling directions. In Fig. 4, the particle channeling in the armchair direction has a flat head leading facet with the longest side of the particle at the head of the channel. Figure 1 shows a particle which has changed from armchair to zigzag channeling direction, and while channeling in the zigzag direction the leading head has an angled facet. The faceted leading face of the particle is further illustrated in Figs. 5 and 6, which show that the leading face is

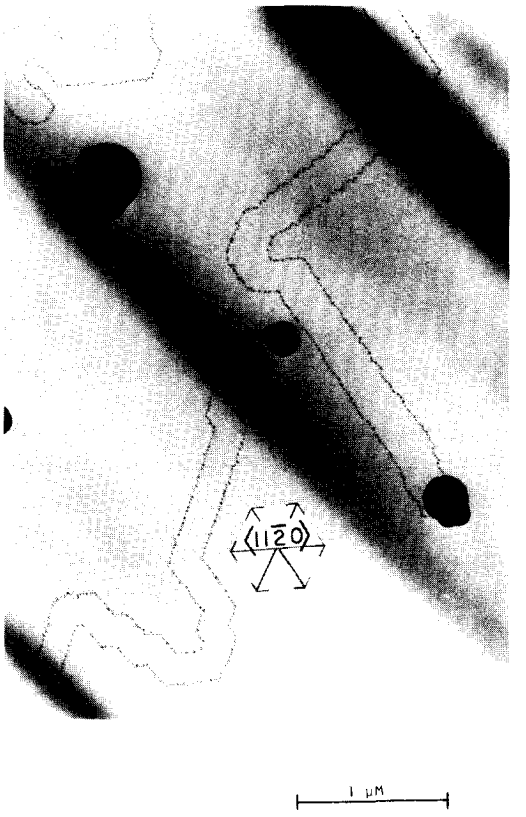

FIG. 2. Platinum particles reacted at 950°C in 0.25 atm hydrogen for 30.0 min. This illustrates a vacancy-originated channel.

FIG. 3. Platinum particles reacted at 850°C in 1.0 atm hydrogen for 45.0 min. This shows vacancy-originated channels crossing paths and illustrates equal channeling depths.

always zigzag orientated regardless of the channeling direction.

Tomita and Tamai (*20*) interpreted the same phenomenon for deep layer channeling in terms of reactivity anisotropy. A more plausible interpretation can be made based on an analysis of the interfacial tensions initially proposed by Baker *et al.* for the Ni/graphite system (*6, 7*).

The balance of the interfacial tensions, as shown in Fig. 7 for the Pt-zigzag face, is

$$\gamma_{\text{zigzag}} = \gamma_{\text{Pt-zigzag}} + \gamma_{\text{Pt}} \cos\theta \qquad (1)$$

where γ is the surface (in contact with gas) or interfacial tension. Likewise for the armchair face:

$$\gamma_{\text{armchair}} = \gamma_{\text{Pt-armchair}} + \gamma_{\text{Pt}} \cos\theta. \qquad (2)$$

The values of γ_{zigzag} and γ_{armchair} were reported to be 4.8 and 5.5 J/m^2, respectively (*21*). Using these values and Eqs. (1) and (2), the condition for the zigzag face to have a stronger wetting interaction is

$$[\gamma_{\text{Pt-zigzag}}] < [\gamma_{\text{Pt-armchair}} - 0.7\ \text{J/m}^2]. \qquad (3)$$

The above condition must hold in order for the Pt particle to maintain contact with the zigzag $\{10\bar{1}1\}$ face of graphite, as observed in the monolayer channeling.

An interesting observation found only in monolayer channeling experiments can be seen in Fig. 8. Here a particle was found to produce a large hexagonal pit at 900°C. Figure 9 shows this to be the beginning of a vacancy-originated channel. The particle

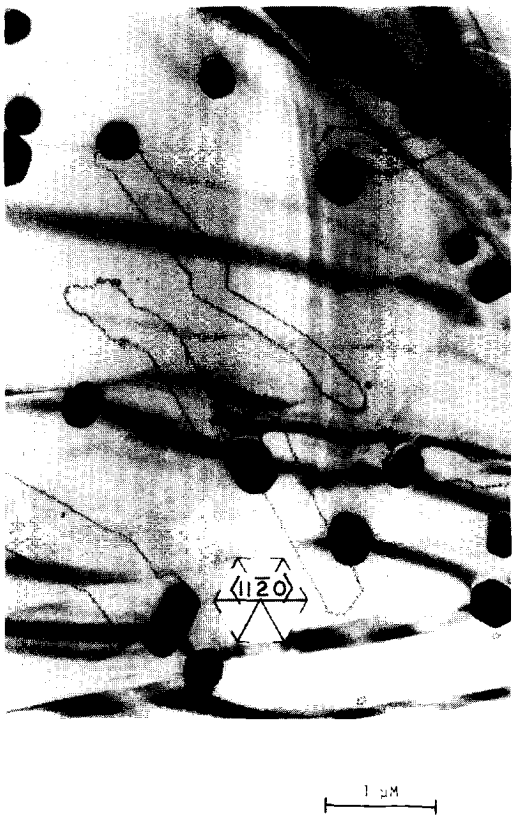

FIG. 4. Platinum particles reacted at 850°C in 1.0 atm hydrogen for 45 min. This shows particles channeling in the armchair direction with a flat head facet at the leading edge of the channel.

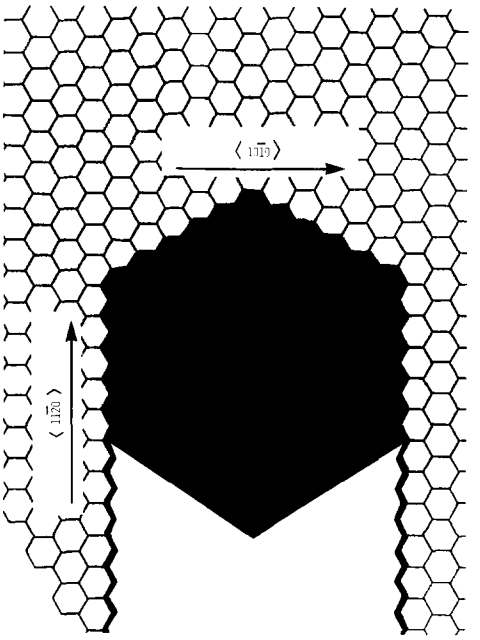

FIG. 5. Schematic representation of particles channeling in the zigzag direction.

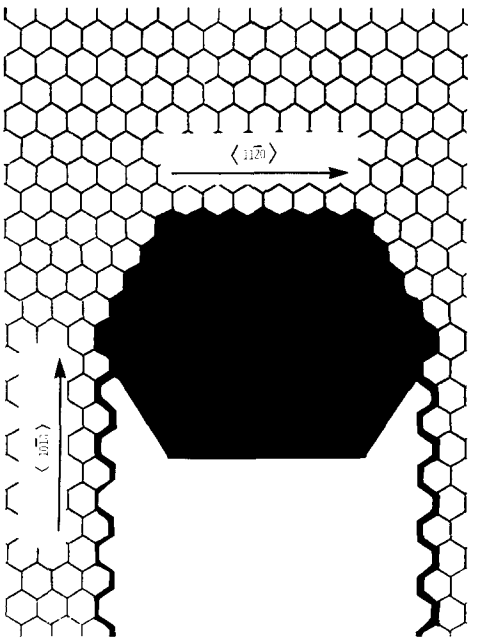

FIG. 6. Schematic representation of particles channeling in the armchair direction.

produces a larger hexagonal pit width than that of the resulting channel. The particle wetting the zigzag face (preferentially) is the driving force for particle movement, and the larger initial hexagonal pit can also be explained. At first the particle is reacting against six zigzag faces, thus being pulled in six directions until this is no longer stable. Then the particle starts channeling, which slightly elongates the particle and causes the channel to be narrower. This larger initial hexagonal pit was not found to occur below 900°C where the particle is more rigid. The particle movement in this monolayer channeling system exhibits a measure of the strength of the metal–support interaction since the step is only 3.35 Å high while the average particle is 3000 Å in diameter.

Rates and Mechanism of Monolayer Channeling

The monolayer channeling rates at 950°C are summarized in Fig. 10. The only meaningful rate expression was based on the surface area of the channeling Pt particle. The rates were calculated from the channel lengths by assuming that (1) Pt particles were hemispherical and (2) all channels were initiated at time zero, i.e., when the hydrogen was introduced. The latter assumption was a valid one as Baker *et al.* (*10*) noted that, in the Pt/graphite/H_2 system, platinum particle movement on the basal plane did not occur at temperatures below 1000°C. Thus monolayer channeling occurs only when the Pt particles are initially in contact with lattice vacancies and steps.

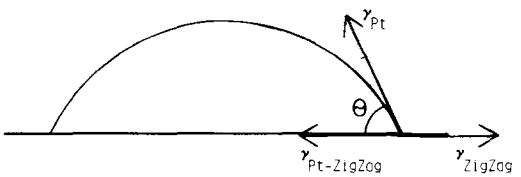

FIG. 7. Balance of interfacial tensions, showing the condition for wetting.

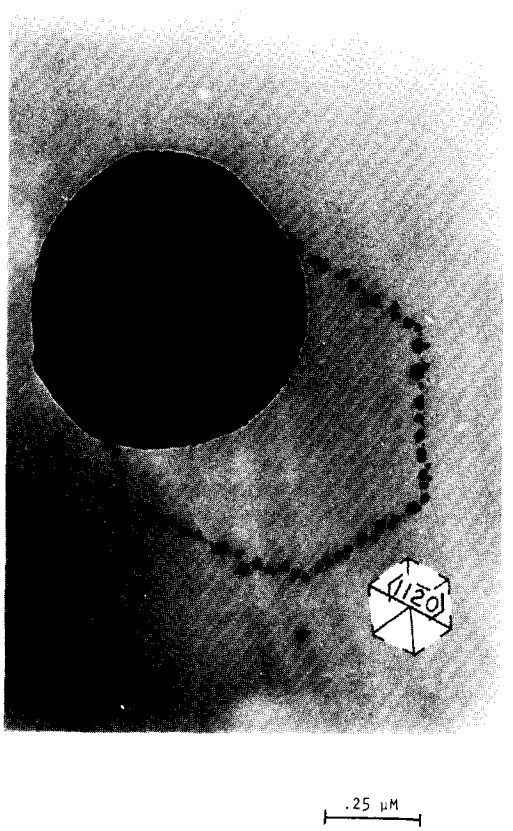

FIG. 8. Platinum particle reacted at 900°C in 1.0 atm hydrogen for 31 min, illustrating vacancy as the origin of a monolayer channel.

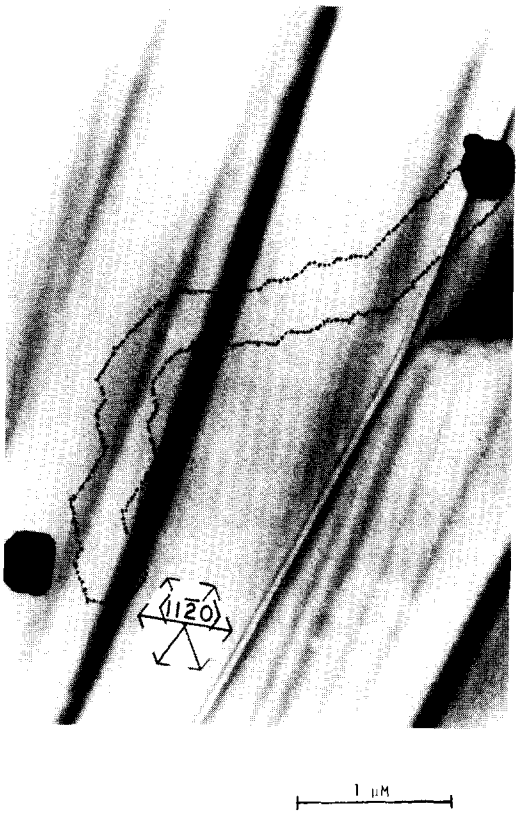

FIG. 9. Platinum particle reacted at 950°C in 1.0 atm hydrogen for 30 min. The initial hexagonal pit of the vacancy-originated channel has a larger width than the resulting channel.

The rate data show two important results:

(1) The Pt-catalyzed reaction is zero order in hydrogen partial pressure.

(2) The rate is limited by the exposed Pt surface.

These two results have been observed, separately, for the Pt/graphite/H_2 system by other experimental techniques. The zero-order hydrogen dependence was reported by Holstein and Boudart (*2*) based on bulk rate measurement at temperatures below 700°C using powdered graphite (a carbon black) impregnated with highly dispersed Pt. The dependence of rates on Pt dispersion was not reported in their study. In the deep layer channeling studied with *in situ* TEM, a Pt-surface limited rate was reported by Keep *et al.* (*5*) for the Ni/graph-

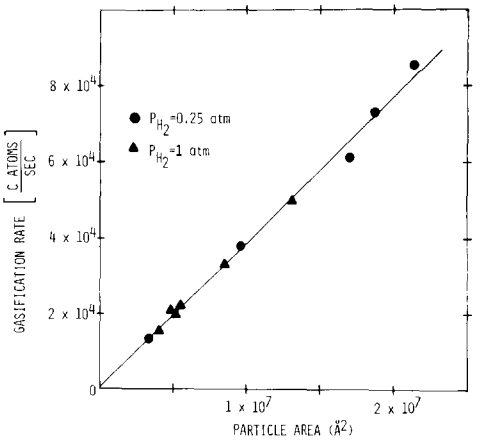

FIG. 10. For platinum particles in the monolayer channeling mode of catalysis at 950°C the gasification rate, in carbon atoms per second per channel, is plotted versus the particle surface area exposed to the gas phase.

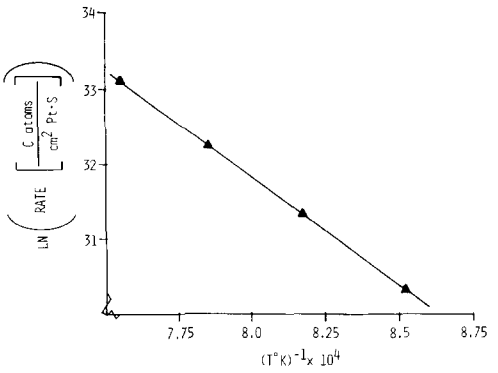

FIG. 11. Temperature dependence of the Pt-catalyzed monolayer channeling rate.

ite/H_2 system in which a linear dependence of rate (of carbon gasified) per particle on the particle area was obtained. The same dependence is also seen in the results of Baker *et al.* for Ni (*6, 7*) and Pt (*10*) systems. The hydrogen pressure dependence was, however, not studied in the *in situ* TEM experiments (the pressure was fixed at 1 Torr). Based on the above comparison, a similarity in the reaction mechanism is already evident among monolayer channeling, deep layer channeling, and bulk measurement. Further comparisons will be given below.

The temperature dependence of the monolayer channeling rate is given in Fig. 11, from which an activation energy of 57 kcal/mole is obtained. The activation energy of 62 kcal/mole was reported by Holstein and Boudart (*2*), and 60 kcal/mole by Baker *et al.* (*10*).

Based on the rate data, conclusions can be drawn regarding the mechanism of the Pt catalyzed monolayer channeling. Several mechanisms can be eliminated as the rate-limiting step based on the linear rate dependence on the particle area shown in Fig. 10. These include: (1) the Pt-catalyzed carbon–carbon bond breakage, (2) H spillover on Pt followed by reaction at the Pt–carbon interface, and (3) direct reaction between H_2 and carbon at the Pt–carbon interface. For any of (1)–(3) to be the rate-limiting step, the channeling speed would have to be independent of particle size. The hydrogen spillover mechanism also contradicts the observed zero-order hydrogen pressure dependence, as pointed out by Holstein and Boudart (*2*). Further evidence against the hydrogen spillover mechanism can be obtained in a calculation of the methane production rate based on the rate of chemisorption of hydrogen on Pt, assuming four chemisorbed H result in a CH_4 molecule. Brennan and Fletcher (*22*) reported a sticking coefficient of 0.24 for the chemisorption of hydrogen on Pt at 1500°C. (The gas-phase hydrogen atom production rate reported by these authors should not be used for the purpose of this calculation (*9*).) Using this sticking coefficient, the CH_4 production rate in the Pt-catalyzed carbon–hydrogen reaction at 950°C would be 6.7×10^{22} molecules/(s × cm^2 Pt), assuming a hydrogen spillover mechanism. This value is nine orders of magnitude higher than our experimental value, 4×10^{13} molecules/(s × cm^2 Pt) (*16*).

The only plausible mechanism for the Pt monolayer channeling is illustrated in Fig. 12. Carbon dissolves in Pt and diffuses through it (and on the Pt surface) to the Pt surface where the methanation reaction takes place. An Eley–Rideal mechanism for the reaction between surface carbon and

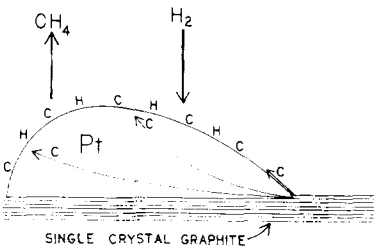

FIG. 12. Schematic representation of the mechanism for monolayer channeling in the Pt-catalyzed C–H_2 reaction. Pt wets the zigzag edge preferentially (with a smaller contact angle than on the other planes), providing the forces for movement. Surface reaction on Pt between C and H is the rate-limiting step for the particle sizes used in this study. (Sizes of Pt particles and graphite layers are not drawn to scale.)

gas-phase H_2 is not important judging from the zero-order hydrogen dependence. For the particle size range observed in this study, i.e., below 5,000 Å diameter, diffusion of carbon is not the rate-limiting step. The rate-limiting step is the surface reaction between surface carbon and chemisorbed hydrogen on Pt, at their respective equilibrium amounts.

An interesting comparison between the rates of monolayer channeling, deep-layer channeling, and bulk measurement can be made if the above mechanism is operative in all modes of the Pt-catalyzed reactions. The bulk rate of Holstein and Boudart (*2*) at 640°C (the highest temperature at which rates are given) is 8.4 ng/m^2/s, or 5.2×10^{10} C atoms/s/cm^2 Pt. The depths of the deep channels were not measured in the study by Baker *et al.* (*10*). The particle sizes were smaller, mainly in the range between 300 and 500 Å diameter. Assuming channel depths of 10 to 15 graphite layers (33.5–50.2 Å), their rates would extrapolate to 1.0–1.5 $\times 10^{11}$ C atoms/s/cm^2 Pt at 640°C. Our monolayer channeling rates, extrapolated to the same temperature, gives 3.9×10^{10} C atoms/s/cm^2 Pt. This comparison infers that the same mechanism is operative in all three modes of catalytic action. The fixed-bed powder reaction by Holstein and Boudart was at low temperatures where Pt does not wet graphite. It was likely, however, that pitting and channeling on the multilayer edges of the small graphite crystals took place in the reaction (simply by gravity).

The rates reported here should correlate with the rates of the methanation reaction (from CO + H_2), since the generally accepted mechanism of this reaction is the hydrogenation of the "carbidic" carbon on the metal surface. Agreement of kinetic data between the two reactions (Metal/graphite/H_2 and Metal/CO + H_2) would indicate a common rate-limiting step. Unfortunately, kinetic data for Pt-catalyzed methanation are not available (since methanol is the predominant product for Pt). Kinetic data are available, however, for both reactions catalyzed by Ni. The activation energy for the Ni catalyzed carbon–hydrogen reaction is much lower than that catalyzed by Pt. A value of 23 kcal/mole was reported for deep-layer channeling (*6*) and 25 kcal/mole (*3*) was reported for bulk (mixed powder) reaction. Goodman *et al.* (*23*) reported rate data of the hydrogenation reaction of the Ni (100) surface precarbided by CO. The activation energy (at temperatures below 372 K) was 21 kcal/mole, in agreement with the Ni-catalyzed carbon–hydrogen reaction data. Comparison of the rate data is difficult due to the widely different temperatures used for these two reactions. Nonetheless, rates based on per Ni surface area extrapolated to the same temperature for the two different reactions fall within one order of magnitude: 1.2×10^{15} C atoms/s/cm^2 Ni from the deep-layer channeling data (*5*), 2.7×10^{15} C atoms/s/cm^2 Ni from the bulk reaction data for Ni/carbon black/H_2 (*8*), and 2×10^{16} C atoms/s/cm^2 Ni from the methanation data of Goodman *et al.* (*23*), all extrapolated to 1035 K.

CONCLUSIONS

(1) The rate-limiting step in the Pt-catalyzed graphite–hydrogen reaction by monolayer channeling is the surface reaction on Pt between surface carbon and chemisorbed hydrogen. The carbon is supplied by the breakage of C—C bonds at the interface between Pt and zigzag graphite edges followed by diffusion, neither of the two steps are rate-limiting for Pt particle sizes below 5000 Å.

(2) The particle movement is driven by adhesion forces between Pt and edge planes of graphite. The preferred wetting edge plane is the $\{10\bar{1}1\}$ zigzag plane and the following relationship holds for the interfacial tensions:

$$\gamma_{\text{Pt-zigzag}} < (\gamma_{\text{Pt-armchair}} - 0.7 \text{ J/m}^2)$$

(3) Comparison of the monolayer channeling data with those in the literature on multilayer channeling and bulk rate mea-

surement (using mixed powders) indicates that the same mechanism is operative in all three modes of catalytic action. A further comparison of the kinetic data for the catalyzed C/H_2 reaction and for the methanation reaction (from $CO + H_2$) suggests the likelihood of a common rate-limiting step.

ACKNOWLEDGMENT

This work was supported by the National Science Foundation under Grant CBT-8507525.

REFERENCES

1. Baker, R. T. K., Lund, C. R. F., and Chludzinski, J. J., Jr., *J. Catal.* **87,** 255 (1984).
2. Holstein, W. L., and Boudart, M., *J. Catal.* **72,** 328 (1981).
3. (a) Tomita, A., and Tamai, Y., *J. Catal.* **72,** 293 (1972); (b) Tomita, A., Sato, N., and Tamai, Y., *Carbon* **12,** 143 (1974).
4. McKee, D. W., *in* "Chemistry and Physics of Carbon" (P. L. Walker, Jr. and P. A. Thrower, Eds.), Vol. 16, p. 1. Dekker, New York, 1981.
5. Keep, C. W., Terry, S., and Wells, M., *J. Catal.* **66,** 451 (1980).
6. Baker, R. T. K., and Sherwood, R. D., *J. Catal.* **70,** 198 (1981).
7. Baker, R. T. K., Sherwood, R. D., and Derouane, E. G., *J. Catal.* **75,** 382 (1982).
8. Grigor'ev, A. P., Lifshits, S. K., and Shamaev, P. P., *Kinet. Catal.* **18,** 948 (1977).
9. Rewick, R. T., Wentrcek, P. R., and Wise, H., *Fuel* **53,** 274 (1974).
10. Baker, R. T. K., Sherwood, R. D., and Dumesic, J. A., *J. Catal.* **66,** 56 (1980).
11. Hennig, G. R., *in* "Chemistry and Physics of Carbon" (P. L. Walker, Jr. Ed.), Vol. 2, p. 1. Dekker, New York, 1966.
12. Thomas, J. M., *Carbon* **8,** 413 (1970).
13. Yang, R. T., *in* "Chemistry and Physics of Carbon" (P. A. Thrower, Ed.), Vol. 19, p. 163. Dekker, New York, 1984.
14. Wong, C., "A Study of Carbon Gasification by Electron Microscopy," Ph.D. dissertation. State University of New York, Buffalo, N.Y., 1983.
15. Yang, R. T., and Wong, C., *Science* **214,** 437 (1981).
16. Goethel, P. J., M.S. thesis. State University of New York, Buffalo, N.Y., 1986.
17. McKee, D. W., and McCarroll, B., *Carbon* **9,** 301 (1971).
18. Hennig, G. R., *J. Chem. Phys.* **40,** 2877 (1964).
19. Wong, C., and Yang, R. T., *Carbon* **20,** 253 (1982).
20. Tomita, A., and Tamai, Y., *J. Phys. Chem.* **78,** 2254 (1974).
21. Abrahamson, J., *Carbon* **11,** 337 (1973).
22. Brennan, D., and Fletcher, P. C., *Trans. Faraday Soc.* **56,** 1662 (1960).
23. Goodman, D. W., Kelley, R. D., Madey, T. E., and White, J. M., *J. Catal.* **64,** 479 (1980).